THE JOURNAL OF PHYSICAL CHEMISTRY B

Article

pubs.acs.org/JPCB

Mixtures of Supported and Hybrid Lipid Membranes on Heterogeneously Modified Silica Nanoparticles

Aundrea R. Piper-Feldkamp,[†] Maria Wegner,[‡] Peter Brzezinski,[‡] and Scott M. Reed*[,†]

[†]Department of Chemistry, University of Colorado Denver, Campus Box 194, P.O. Box 173364, Denver, Colorado 80217-3364, United States

[‡]Department of Biochemistry and Biophysics, Stockholm University, Svante Arrhenius väg 16, SE-106 91, Stockholm, Sweden

Supporting Information

ABSTRACT: Simple supported lipid bilayers do not accurately reflect the complex heterogeneity of cellular membranes; however, surface modification makes it possible to tune membrane properties to better mimic biological systems. Here, 3-[2-(2-aminoethylamino)ethylamino]propyl-trimethoxysilane (DETAS), a silica modifier, facilitated formation of supported lipid bilayers on silica nanoparticles. Evidence for a stable supported bilayer came from the successful entrapment of a soluble fluorophore within an interstitial water layer. A fluorescence-quenching assay that utilized a pore-forming peptide was used to demonstrate the existence of two separate lipid leaflets. In this assay, fluorescence was quenched by dithionite in roughly equal proportions prior to and after addition of melittin. When a hydrophobic modifier, octadecyltriethoxysilane, was codeposited on the nanoparticles with DETAS, there was a decrease in the amount of supported bilayer on the nanoparticles and an increase in the quantity of hybrid membrane. This allowed for a controlled mixture of two distinct types of membranes on a single substrate, one separated by a water cushion and the other anchored directly on the surface, thereby providing a new mimic of cellular membranes.

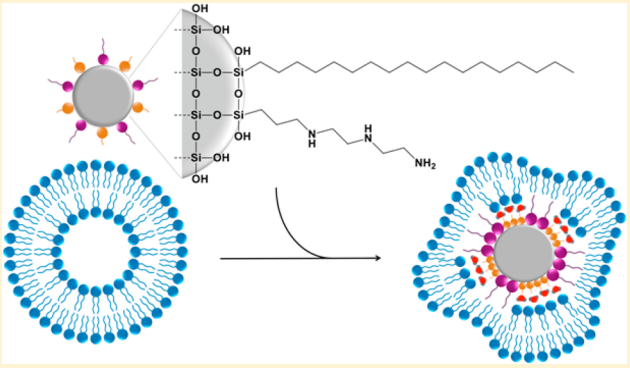

INTRODUCTION

In living systems, complex heterogeneous lipid bilayers serve to compartmentalize cellular functions and are critical to mediating signaling, transport, and other biological functions by providing defined interfaces for recognition and interaction.[1] Supported lipid bilayers are a well-established mimic of biological membranes and consist of two opposing leaflets of lipids supported at the aqueous interface of a hydrophilic solid.[2−4] These mimics are generally formed by liposome rupture upon contact with a planar or colloidal surface, with lipids then spreading to enclose an interstitial water layer.[5−7] Interest in supported lipid bilayers stems primarily from their usefulness as simplified model systems for characterizing the structure, assembly, dynamics, and functions of biological membranes.[8−10] Supported membranes are also important in the design of biocompatible surfaces and biosensors and as analytical platforms for assaying protein−membrane interactions.[9,11,12]

Although supported lipid bilayers are powerful as simplified models, large discrepancies in lipid diffusion rates between supported bilayers and true cellular membranes have been reported.[13] Fluorescence tracking measurements have revealed compartmentalization of lipids that lowers the diffusion rate, and it has been proposed that this compartmentalization is caused by attachement of the membrane to the cytoskeleton.[14] Membrane-spanning proteins can form semipermeable boundaries that permit rapid diffusion within domains while slowing diffusion between domains.[14,15] This picket fence structure alters lipid mobility because the membrane skeleton influences the movements of membrane molecules.[14,16] New model systems are needed that better mimic this compartmentalized behavior of biological membranes.

Changes to the surface chemistry of solid supports can alter the lipid membrane interfaces, thereby modifying the physical properties of membranes. This provides a simple and effective means to control membrane properties, including spatial molecular distributions, compositional heterogeneity, lateral tension, packing density, diffusion rates, curvature, and membrane morphology.[17] For example, hydrophobic surface modifiers have been used on both planar[18−20] and nanoparticle surfaces[21−26] to create hybrid membrane structures using both silica and gold surfaces. Advances in patterning and surface modification methods[27,28] have allowed for the fabrication of surfaces with chemical and topographical variation at micrometer to nanometer length scales. Mixtures of supported and hybrid membranes (Scheme 1) could function to mimic the

Received: August 21, 2012
Revised: January 4, 2013
Published: February 6, 2013

dx.doi.org/10.1021/jp308305y | J. Phys. Chem. B 2013, 117, 2113−2122

Scheme 1. Schematic Depiction of a Heterogeneous Distribution of DETAS and ODTS around a SiNP, Resulting in a Mixture of Hybrid Membrane and Supported Bilayer Regions[a]

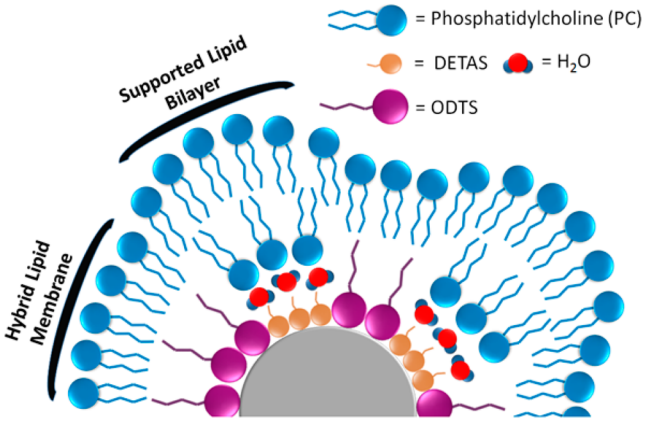

[a]Illustration is not drawn to scale.

picket fence structure of membranes, and patterning has allowed the creation of surfaces with coexisting regions of supported lipid bilayers and hybrid membranes on the same substrate.[12,18,20,29−33] Although nanoparticle templates have been used for both supported[25,34] and hybrid membranes[21,23,25] individually, they have not been used to prepare nanoparticles containing both types of membranes. Creating such mimics on nanoparticle templates would allow for additional methods of studying the membranes and their interactions with proteins.

We explored methods of preparing silica nanoparticle (SiNP) surfaces with a heterogeneous combination of hydrophilic and hydrophobic silane modifiers, DETAS and octadecyltriethoxysilane (ODTS). These two trialkoxysilanes were anchored on the SiNPs at different ratios, and the SiNPs were then coated with L-α-phosphatidylcholine (PC). Both the silane-modified SiNPs and the PC coating were studied using thermogravimetric analysis (TGA) to quantify the amount of each silane on the surface and to determine how much PC was required to coat a single SiNP. Fluorophore release and quenching studies were employed to characterize the PC-coated SiNPs. Increasing the fraction of hydrophobic silane on the SiNP surface led to an increasing proportion of hybrid membrane.

EXPERIMENTAL METHODS

Materials. 3-[2-(2-Aminoethylamino)ethylamino]propyltrimethoxysilane (DETAS) was from Acros Organics (Pittsburgh, PA); anhydrous calcium chloride, octadecyltriethoxysilane (ODTS), 3-aminopropyltriethoxysilane (APTES), and sodium dithionite were from Alfa Aesar (Ward Hill, MA). A 1 M solution of 2-amino-2-hydroxymethyl-propane-1,3-diol (TRIS), pH 8.0, was from Ambion (Grand Island, NY); soy PC and 1-palmitoyl-2-[12-[(7-nitro-2-1,3-benzoxadiazol-4-yl)-amino]dodecanoyl]-*sn*-glycero-3-phosphocholine (NBD-PC) were from Avanti Polar Lipids (Alabaster, AL). Ammonium hydroxide (28−30%), *N*-2-hydroxyethylpiperazine-*N*′-2-ethane sulfonic acid (HEPES), pH 6.5, and ethanol (190 proof) were from VWR Scientific (Radnor, PA); glacial acetic acid and sodium chloride were from Mallinckrodt Chemicals (Phillipsburg, NJ); chloroform was from VWR Scientific (Radnor, PA) and was filtered through basic alumina (Dynamic Adsorbents, Nocross, Georgia) prior to use. Tetraethylorthosilicate (TEOS) was from Sigma Aldrich (St. Louis, MO), and Sephadex G-100 Superfine was from Pharmacis Fine Chemicals (Uppsala, Sweden). Ultrapure water (18 MΩ) was from a Milli-Q Integral Water Purification System by EMD Millipore (Billerica, MA).

Synthesis of Silica Nanoparticles. Spherical SiNPs were synthesized using the Stöber method.[35] Briefly, ethanol (40 mL) and ammonium hydroxide (1.0 mL) were stirred for 7 min in a glass flask before TEOS (0.5 mL) was added. The resulting mixture was stirred overnight at 30−35 °C. The synthesized SiNPs were purified by centrifugation (9400*g*, 10 min) using an Eppendorf 5424 Microcentrifuge (Eppendorf International, Hamburg, Germany). The pellet was resuspended by sonication in ethanol. This purification was repeated three times to remove unreacted precursors and impurities. The diameter of the SiNPs was 107 ± 3 nm by dynamic light scattering (DLS).

Functionalization of SiNPs. Ten milliliters of a 5 wt % SiNP solution in ethanol was added to a mixture of DETAS and ODTS, keeping the total silane concentration at ∼0.1 volume percent. All input ratios are given as a mole percentage of DETAS, where the remaining fraction is ODTS. The resulting solutions were diluted in ethanol to a total volume of 50 mL, and the reaction was stirred while refluxing overnight. The resulting functionalized SiNPs were washed by centrifugation (9400*g*, 10 min) three times with 190 proof ethanol (35 mL) then once with Milli-Q water (35 mL). The average diameter of the functionalized SiNPs was ∼113 ± 2 nm by DLS.

Thermogravimetric Analysis. TGA was performed on a TA Instruments Q50 Thermogravimetric Analyzer (New Castle, DE). The platinum pan was loaded with ∼6−10 mg of dry sample or 60−80 mg of wet sample, and the temperature was increased to 800 °C at a ramp rate of 2 °C/min. Dry samples were prepared by overnight evaporation of solvent in an oven at 110 °C. PC-coated samples were analyzed after purification, without drying.

The weight loss for each sample that was attributable to DETAS pyrolysis was estimated using the weight loss ratio (WLR) of loss that occurred from 150 to 440 °C to the loss that occurred from 440 to 800 °C. For SiNP samples containing both silanes, the fraction of DETAS was calculated from these values by referencing samples known to contain exclusively DETAS or ODTS using

$$f_{\mathrm{DETAS}} = \left(\frac{\mathrm{WLR_{SiNP}} - \mathrm{WLR_{ODTS}}}{\mathrm{WLR_{DETAS}} - \mathrm{WLR_{ODTS}}} \right) \quad (1)$$

where $\mathrm{WLR_{SiNP}}$ is the weight loss ratio for a given functionalization, $\mathrm{WLR_{ODTS}}$ is the weight loss ratio for 100% ODTS SiNPs, and $\mathrm{WLR_{DETAS}}$ is the weight loss ratio for 100% DETAS SiNPs.

Preparation of SiNP-Supported Lipid Bilayers. Stock solutions of PC (4 mM) were prepared in chloroform. Lipid films were dried by evaporation of the solvent under a stream of nitrogen, followed by overnight vacuum at room temperature. The samples were kept at −20 °C prior to use. The lipid films were redispersed in either HEPES buffer (10 mM HEPES, 50 mM NaCl, 2 mM $CaCl_2$) or TRIS buffer (10 mM TRIS, 50 mM NaCl, 2 mM $CaCl_2$). The resulting cloudy solutions were sonicated in a cuphorn sonicator (Branson Sonifier 450, Branson Ultrasonics, Danbury, CT) for 15 min at 70% power output. Sonication was followed by extrusion using a Mini Extruder (Avanti Polar Lipids, Alabaster, AL) with a 200 nm

dx.doi.org/10.1021/jp308305y | J. Phys. Chem. B 2013, 117, 2113−2122

pore size polycarbonate filter. Approximately 1 mL of sonicated lipid solution was passed through the membrane at least 15 times, resulting in a clear solution. The liposome diameter (192 ± 5 nm) was measured by DLS. Adsorption of lipids onto the SiNPs was accomplished by stirring an aqueous solution of purified SiNPs with an equal volume of sonicated, extruded PC liposomes (3 mM) for 2 h at room temperature. The PC-coated SiNPs were centrifuged (9400*g*, 10 min), and the supernatant was discarded. Additional buffer was added, and these washing steps were repeated 5 times. After the final centrifugation, the sample was redispersed in 1 mL of HEPES or TRIS buffer for fluorescence measurements or in water for TGA analysis.

The weight loss attributed to PC on the SiNP was determined by subtracting the weight loss for an uncoated SiNP from the PC-coated SiNP. Then the relative PC coverage on the SiNP was calculated from the TGA data with reference to the 100% DETAS sample using

$$\%\text{PC coverage} = 100 - \left(\frac{\text{WL}_{\text{DETAS}} - \text{WL}_{\text{SiNP}}}{\text{WL}_{\text{DETAS}}}\right) \times 100 \tag{2}$$

where WL_{DETAS} is the weight percent change for PC pyrolysis on the 100% DETAS sample and WL_{SiNP} is the weight percent change for PC pyrolysis on the given sample. In addition, the predicted PC coverage for a given surface coverage of DETAS was calculated using

$$\%\text{PC} = \frac{(2 \times f_{\text{DETAS}}) + (1 \times (1 - f_{\text{DETAS}}))}{2} \times 100 \tag{3}$$

where f_{DETAS} is the calculated fraction of DETAS from eq 1.

NBD-PC Fluorescence Quenching. Solutions of PC in chloroform were mixed with 1 mol % NBD-PC, formed into liposomes, and coated onto SiNPs using the above methods. Samples were purified by 5 centrifugation washes (9400*g*, 10 min). The lipid distributions were investigated by measuring NBD fluorescence on an LS 55 luminescence spectrometer (Perkin-Elmer, Waltham, MA) with excitation at 475 nm (2.5 nm slit width) and emission recorded at 534 nm (20 nm slit width). The samples were run by collecting baseline fluorescence for 10 min, followed by addition of sodium dithionite in HEPES buffer (final concentration was 5 mM) and mixing. Five minutes after the addition of sodium dithionite, the fluorescence was collected for 15 min and averaged. Melittin was added (final concentration was 1.3 μM) and mixed, followed by fluorescence measurement for 15 min. The mean and standard deviation of fluorescence changes were calculated from five independently prepared and assayed samples.

The change in fluorescence for the outer leaflet (ΔF_1) was calculated as

$$\Delta F_1 = \frac{\text{FI} - \text{FD}}{\text{FI} - \text{FM}} \tag{4}$$

and the change in fluorescence for the inner leaflet (ΔF_2) was calculated as:

$$\Delta F_2 = \frac{\text{FD} - \text{FM}}{\text{FI} - \text{FM}} \tag{5}$$

where FI is the initial fluorescence, FD is the fluorescence after dithionite is added, and FM is the fluorescence after melittin is added.

To calculate the percentage of supported bilayer on each SiNP using fluorescence quenching data, each sample was normalized to the 100% DETAS sample, which is assumed to be an exclusively supported bilayer, using

$$\%\text{SLB} = 100 - \left(\frac{\Delta F2_{\text{SiNP}} - \Delta F2_{\text{DETAS}}}{\Delta F2_{\text{DETAS}}}\right) \times 100 \tag{6}$$

where $\Delta F2_{\text{SiNP}}$ is the decrease in fluorescence for the inner leaflet of the SiNP sample and $\Delta F2_{\text{DETAS}}$ is the decrease for the inner leaflet on the 100% DETAS sample.

Measuring Interstitial Volume. Calcein-loaded liposomes were prepared using dehydrated PC films that were resuspended and extruded in 60 mM calcein dye in TRIS buffer. Adsorption of the liposomes onto the SiNPs was accomplished by stirring purified SiNPs with the calcein-loaded liposomes for 2 h at room temperature using an established method.[36] Samples were then purified using size-exclusion chromatography on a Sephadex G-100 column. The first, salmon-colored, fraction was collected. The SiNPs in this fraction were pelleted by centrifugation (9400*g*, 10 min), washed, and redispersed in 1 mL of TRIS buffer. Samples were excited at 490 nm (2.5 nm slit width), with emission recorded at 513 nm (10 nm slit width). Initial fluorescence was measured for 10 min. Melittin was added to the sample (final concentration of 1.3 μM) with gentle mixing and incubated for 5 min. Fluorescence was measured for 15 min. In other experiments, 3 μL of 10% Triton-X was added in place of the melittin.

The fluorescence measured after release was used to calculate the total interstitial volume,

$$V_{\text{interstitial}} = \frac{[\text{calcein}]_{\text{cuvette}} \times V_{\text{cuvette}}}{[\text{calcein}]_{\text{interstitial}}} \tag{7}$$

where $[\text{calcein}]_{\text{cuvette}}$ is the concentration of calcein obtained from a standard curve, V_{cuvette} is the total sample volume (800 μL), and $[\text{calcein}]_{\text{interestitial}}$ is the concentration of calcein loaded on the SiNP (60 mM).

The interstitial volume per particle was then calculated as

$$V_{\text{SiNP}} = V_{\text{interstitial}} / \frac{\text{siNP}_{\text{total mass}}}{\text{siNP}_{\text{individual mass}}} \tag{8}$$

where the $\text{SiNP}_{\text{individual mass}}$ was calculated from the average SiNP diameter of 113 ± 2 nm and a density of 2.65 g/mL[37] and $\text{SiNP}_{\text{total mass}}$ was the mass of SiNPs in 800 μL of solution (obtained from a TGA experiment).

The thickness of the water layer was then calculated. First, the SiNP volume was combined with the interstitial volume, and the diameter of a sphere needs to be encompassed. This combined volume was found using

$$d_{\text{water}} = 2 \times \sqrt[3]{3V_{\text{total}}/4\pi} \tag{9}$$

where V_{total} is the combination of V_{SiNP} and the volume of an SiNP (calculated from the DLS diameter). Then the thickness of the interstitial water layer was calculated from

$$\text{thickness} = \frac{d_{\text{water}} - d_{\text{SiNP}}}{2} \tag{10}$$

where d_{SiNP} is the average diameter of the SiNPs.

Membrane Stability Assay. PC-coated, calcein-loaded SiNPs were mixed with HEPES buffer to a total volume of 800 μL. Triton-X was added to a concentration ranging from 0 to

dx.doi.org/10.1021/jp308305y | J. Phys. Chem. B 2013, 117, 2113−2122

0.4 mM, and the fluorescence of each was measured for 10 min. Fluorescence background was subtracted and then normalized to 100 for the highest Triton-X concentration. A nonlinear regression was used to calculate the concentration of Triton-X that resulted in a 50% fluorescence intensity increase (F_{50}) of the respective sample using Prism (Graphpad, San Diego, CA). All R^2 values were >0.96.

Dynamic Light Scattering. DLS measurements were performed on a Zeta Sizer Nano S90 (Malvern Instruments, Westborough, MA). Data were recorded for samples with no visible precipitation. Average size was obtained from the intensity distribution.

Statistical Analysis. Statistical significance was evaluated using Student's t test, and a p value of <0.05 was considered as significant.

RESULTS

Thermal Analysis of Functionalized SiNPs. Samples with different functionalization ratios were synthesized by adding different input ratios of DETAS and ODTS (Scheme 2)

Scheme 2. Silanes Used for Functionalization of SiNPs

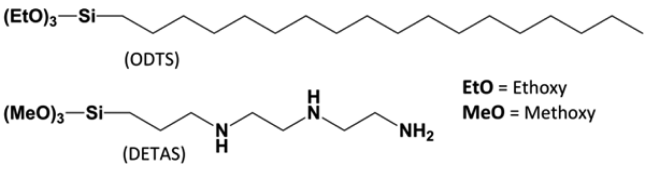

at a total of 0.1 volume percent of silane. The relative amount of each silane on the SiNPs was determined using thermal analysis. Thermal analysis was performed on bare SiNP and SiNPs with nine different functionalization ratios (Figure 1A), and data were normalized to 100% at 150 °C. To better observe differences in weight loss across the series and to identify a cutoff temperature for distinguishing DETAS from ODTS, a differential thermal analysis (DTA) was performed by calculating the rate of change in weight loss at each temperature (Figure 1B). The functionalized SiNPs showed changes in weight loss that varied with the input ratios of silanes used in the synthesis. Samples with 100% DETAS functionalization have three characteristic DTA peaks at approximately 225, 335, and 460 °C.[38] As the input fraction of ODTS in the SiNPs increased, the two lower temperature peaks decreased in intensity while the peak at 460 °C increased (Figure 1B).

To investigate the relationship between the ratio of silanes observed on the surface of the SiNPs by TGA and the input ratio of silanes used in the synthesis, the surface density of silanes was calculated from the TGA data. This was accomplished by calculating the SiNP volume from the average diameter, then converting the volume to an individual nanoparticle mass using the density of SiO_2 as 2.65 g/mL.[37] A surface concentration of 4 silanols per square nanometer was then used to estimate the total number of silanols available on the SiNP.[37] Finally, the number of silanes per surface silanol were calculated (Table 1) using the total silane mass lost, the weighted average of the combustible portion of the molecular weights for each functionalization ratio, and an average SiNP diameter of 113 nm. Bare SiNPs had a 1.97% weight loss over the temperature range measured, indicating only minor condensation of the particles.[35] The 100% DETAS SiNPs had the highest overall weight loss of 11.1% (Table 1). As a higher

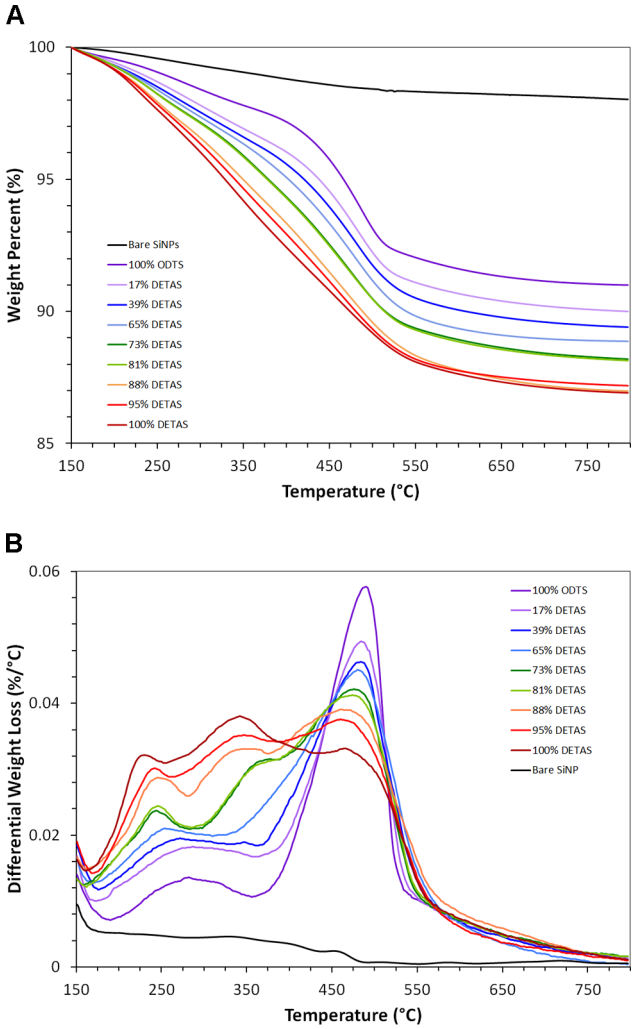

Figure 1. Thermal analysis of SiNPs displayed as (A) the weight percent lost and (B) the differential thermal analysis. Samples were functionalized with 100% DETAS (dark red), 95% DETAS (red), 88% DETAS (orange), 81% DETAS (lime-green), 73% DETAS (dark green), 65% DETAS (light blue), 39% DETAS (blue), 17% DETAS (lavender), 100% ODTS (violet), and bare (black). TGA data was normalized to 100% at 150 °C for each sample.

fraction of ODTS was used, there was a decreasing amount of weight loss.

There is a variation in the weight loss across the series of SiNPs (Figure 1A), with those containing a higher fraction of DETAS showing a greater loss than the ones with more ODTS. This trend is roughly linear with the input moles of silane. The silane density, expressed as silanes per surface silanol group, showed a similar trend, with higher percent DETAS SiNPs having a higher silane coverage, suggesting that DETAS is more prone to deposition of polymerized silane coatings than is ODTS. Alternatively, DETAS may pack more tightly on the surface.

TGA of PC-Coated, Functionalized SiNPs. Thermal analysis of the PC-coated samples was used to investigate how much PC adsorbs to the differently functionalized SiNPs. Thermal analysis of PC-coated 17% DETAS SiNPs (Figure 2, blue) is typical of the PC-coated SiNPs examined; it has two significant weight loss regions at 240−270 and 440−520 °C. The peak in the 240−270 °C region is primarily attributed to PC because it is unique to the PC-coated samples and is

dx.doi.org/10.1021/jp308305y | J. Phys. Chem. B 2013, 117, 2113−2122

Table 1. Characterization of SiNPs by DLS and TGA[a]

input DETAS (volume %)	input DETAS (mol %)	wt % loss ± SD < 440 °C	wt % loss ± SD > 440 °C	total wt % loss ± SD	calculated f_{DETAS}[b]	silanes per surface silanol[c]
100	100	7.5 ± 0.1	3.6 ± 0.1	11.1 ± 0.3	1.00	2.58
90	95	7.1 ± 0.2	3.8 ± 0.2	10.9 ± 0.4	0.88	2.34
80	88	6.7 ± 0.1	4.3 ± 0.2	11.0 ± 0.3	0.67	2.15
70	81	5.7 ± 0.2	4.2 ± 0.2	9.9 ± 0.3	0.55	1.77
60	73	5.7 ± 0.1	4.2 ± 0.2	9.9 ± 0.3	0.54	1.75
50	65	4.9 ± 0.2	4.3 ± 0.1	9.2 ± 0.3	0.39	1.50
25	39	4.3 ± 0.1	4.4 ± 0.1	8.7 ± 0.2	0.30	1.35
10	17	3.6 ± 0.1	4.4 ± 0.1	8.0 ± 0.3	0.20	1.17
0[d]	0	2.4 ± 0.1	4.6 ± 0.2	7.0 ± 0.3	0	0.97

[a]All data reported as mean ± SD, n = 3. [b]Calculated from TGA data using eq 1 with a cutoff of 440 °C. [c]Calculated using average particle diameter of 113 nm. [d]Sample was functionalized with 100% ODTS.

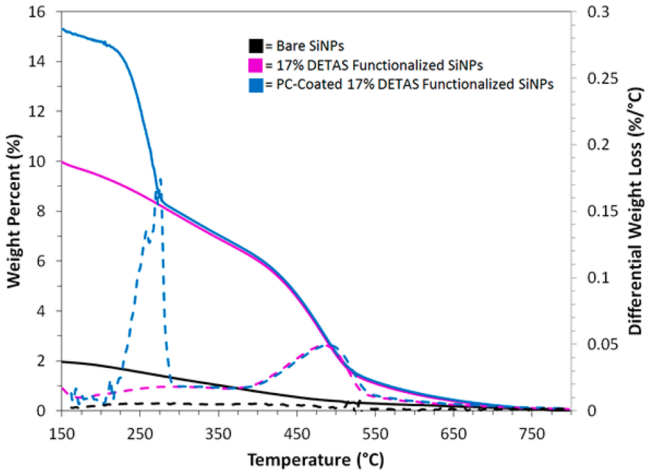

Figure 2. TGA (solid) and DTA (dashed) curves of bare SiNP (black), 17% DETAS-functionalized SiNPs (pink), and PC-coated 17% DETAS-functionalized SiNPs (blue). Data were set to 0 wt % at 800 °C.

consistent with previous studies of PC pyrolysis.[39] The weight loss from a corresponding uncoated SiNP was subtracted from the coated sample to determine the amount of PC on the SiNP (Table 2). Attempts at lipid-coating SiNPs with 100% ODTS functionalization resulted in rapid aggregation in aqueous solutions. Thus, for all experiments involving lipids, 83% ODTS was the highest mole percent used. The significance of the weight percent change from PC loss was compared with the 100% DETAS sample (Table 2).

Table 2. Thermal Analysis of PC-Coated Functionalized SiNPs with Varying Input DETAS %[a]

input DETAS (mol %)	PC wt % loss ± SD	% PC coverage[b]	% PC predicted[c]	p value
100	10.9 ± 1.7	100	100	N/A
95	9.8 ± 1.6	90	94	>0.05
88	9.1 ± 1.4	83	84	>0.05
81	7.9 ± 1.5	72	78	<0.05
73	7.7 ± 1.5	71	77	<0.05
65	7.2 ± 1.4	66	70	<0.01
39	5.9 ± 1.2	54	65	<0.001
17	5.2 ± 1.4	48	60	<0.001

[a]n = 5. Data were compared to 100% DETAS to determine the p value. [b]Compared with the 100% DETAS sample using eq 2. [c]Calculated using eq 3.

In the absence of normalization, each sample has slightly more PC than would be expected on the basis of calculating each leaflet as a sphere of PC using the DLS data to determine the sphere size. That is, the experimental weight loss values (e.g., for 100% DETAS the weight loss was 10.9%) are somewhat higher than the expected weight percent, assuming PC to be a homogeneous spherical shell. This could reflect instrumental error in either the TGA or DLS measurements. In particular, small errors in the diameter measured will have a large influence on the amount of PC calculated as required to coat the SiNPs. Since an alternate explanation is that excess liposomes were bound to the SiNPs, the ability of five wash steps to remove free liposomes[2] was confirmed by a spiking experiment (Supporting Information Figure S3). Another explanation for this increase could be that an additional fraction of interdigitated PC is present on the SiNPs that is exclusively in the outer leaflet, as previously reported for PC-coated SiNPs.[40,41]

The amount of PC adsorbed on the functionalized SiNPs decreased with increasing coverage of hydrophobic ODTS. This can be rationalized as a mixture of supported and hybrid membrane on the surface (Scheme 1). The relative percent PC coverage was calculated by normalization to the 100% DETAS SiNPs, thus providing an estimate of how much less PC was required due to the presence of ODTS on the SiNP. This decrease in the amount of PC required is consistent with a model in which the amount of ODTS present determines the amount of hybrid membrane present. ODTS regions would be coated with a hybrid membrane that has only one leaflet of PC, whereas DETAS regions would have a two-leaflet PC bilayer. For comparison, a prediction was made as to the amount of PC needed on the basis of the assumption that DETAS regions would be coated with 2 PC leaflets and the ODTS regions with 1 PC leaflet using eq 3.

NBD-PC Fluorescence Quenching. To measure the lipid distribution between the inner and outer leaflets of the membrane at each functionalization ratio, the functionalized SiNPs were coated using liposomes doped with NBD-PC. Sodium dithionite, which quenches the NBD fluorescence by chemically reducing the dye,[39] was added to the PC-coated SiNPs. The fluorescence of each sample was measured and compared with its initial fluorescence. Melittin or Triton-X was added to the sample to expose the inner leaflet lipids to the dithionite quencher. Melittin was used to create membrane pores,[42−45] and Triton-X was used to solubilize the PC from the SiNPs. A representative plot of fluorescence is shown for a sample of PC-coated 100% DETAS-functionalized SiNPs

dx.doi.org/10.1021/jp308305y | J. Phys. Chem. B 2013, 117, 2113−2122

(Figure 3). Fluorescence intensity drops were complete within 5 min of dithionite or melittin addition. Changes in fluorescence were calculated using eqs 4 and 5 (Table 3). Controls were performed with both Triton-X plus dithionite as well as dithionite only (see Supporting Information Figure S1).

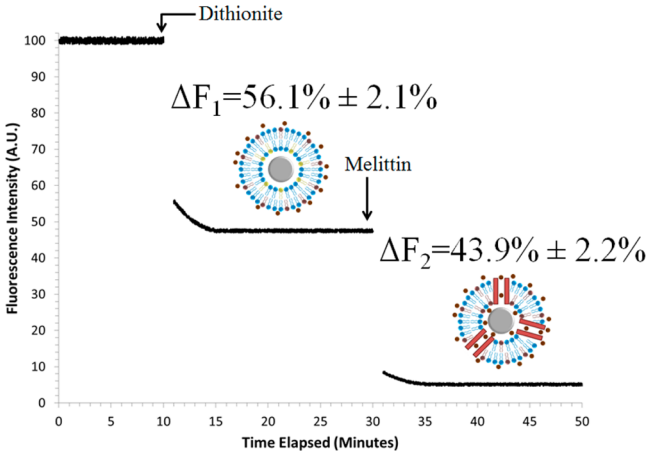

Figure 3. Dithionite quenching of PC/NBD-PC-coated SiNPs, functionalized with 100% DETAS. Outer leaflet fluorescence was quenched by the addition of sodium dithionite (5 mM), followed by melittin (1.3 μM). The outer leaflet (ΔF_1) and inner leaflet (ΔF_2) fluorescence quenching was calculated using eqs 4 and 5. Data are presented as mean ± SD, n = 5. Plot is representative of multiple experiments.

Table 3. Inner and Outer Leaflet Lipid Distribution and Fraction of Supported Bilayer Calculated from NBD Quenching Data[a]

input DETAS (mol %)	% quenched (outer leaflet)[b]	% quenched (inner leaflet)[c]	calculated % SLB[d]
100	56.1 ± 2.1	43.9 ± 2.2	100
95	58.4 ± 1.9	41.6 ± 1.7	95
88	59.8 ± 2.0	40.2 ± 1.7	92
81	61.9 ± 2.0	38.1 ± 2.1	87
73	64.4 ± 2.4	35.6 ± 2.2	81
65	66.1 ± 2.6	33.9 ± 2.6	77
39	73.4 ± 2.2	26.6 ± 2.4	61
17	79.7 ± 2.1	20.3 ± 2.2	46
bare	53.0 ± 2.1	47.0 ± 1.9	N/A

[a]Mean ± SE, n = 5. [b]Calculated using eq 4. [c]Calculated using eq 5. [d]Calculated using eq 6. SLB = supported lipid bilayer.

The same technique was employed for each functionalized SiNP (Table 3). For the 100% DETAS SiNPs, 56% quenching occurred in the first step (outer leaflet) and 44% in the second step (inner leaflet), consistent with a symmetric supported bilayer structure. As ODTS functionalization increased, the percentage of lipids present on the inner layer decreased. At the highest ODTS fraction, the lipids are distributed with 80% in the outer leaflet and 20% in the inner leaflet. This is consistent with a mixture of supported and hybrid membrane regions on the functionalized SiNPs (Scheme 1).

A second method of estimating the fraction of supported and hybrid membrane on the SiNPs was based on the quenching data. The fraction of supported bilayer was calculated using eq 6 (Table 3), and the higher the input ODTS, the less supported bilayer there was on the SiNPs. The values obtained from this calculation are comparable to those obtained from the TGA data (Table 2).

Interstitial Volume Decreases with Increasing Fraction of Hydrophobic Coating. To investigate the relationship between interstitial volume and input functionalization ratios, SiNPs were incubated with PC liposomes that had been resuspended in a self-quenching calcein solution (60 mM) (Scheme 3). After purification, the PC-coated SiNPs were porated or lysed to determine the amount of calcein solution entrapped in the interstitial layer. Melittin has been shown to form a 2.5−3.0 nm diameter pore,[45] large enough to allow passage of calcein, which has an estimated diameter of 1.2 nm.[46] Release of the entrapped calcein resulted in a roughly 40-fold dilution of the dye into the cuvette, thereby decreasing the concentration to a level where it fluoresces.

The calcein concentration in the cuvette was obtained from the measured fluorescence intensity after release and was used to determine the interstitial volume. This was converted to an interstitial volume per SiNP using eqs 7, 8, and 9 and a thickness of the interstitial water layer using eq 10 (Table 4). The more ODTS on the surface of the SiNPs, the smaller the interstitial volume was. PC-coated, 100% DETAS-functionalized SiNPs showed a difference in water layer thickness that was not significantly different from the PC-coated bare SiNP control. Functionalization with the PC-coated, 17% DETAS SiNPs showed a decrease in the water layer thickness by ∼86% relative to the PC-coated bare SiNPs. A trend of decreasing fluorescence can be observed with decreasing water layer thickness as the DETAS percentage decreases (Table 4, Figure 4).

Bilayer Stability Assay. To examine the stability of the PC-coated functionalized SiNPs, calcein-loaded SiNPs were exposed to increasing concentrations of melittin or Triton-X (Scheme 3). After measuring the fluorescence after release, F_{50} values were calculated as the concentration of Triton-X that resulted in a 50% increase in fluorescence intensity (Figure 5). The stability of 100% DETAS-functionalized SiNPs was significantly lower than the 17% DETAS functionalized SiNPs, with F_{50} values of 0.092 and 0.133 mM, respectively, and this change was statistically different as evaluated by a Student's t test.

DISCUSSION

The surface chemistry required for preparing supported bilayers and hybrid lipid membranes differs, making it a challenge to identify conditions that are compatible with both types of membrane. Supported bilayers can be formed directly on hydrophilic surfaces, such as the silanol coating of unmodified silica.[2,3,40,41,47,48] In contrast, hybrid membranes or tethered membranes[49] are formed on hydrophobic surfaces. For example, alkanethiol monolayers have been used as hybrid membrane supports on planar gold[19] and on gold nanoparticles.[21−23] Similarly, silica nanoparticles have been made hydrophobic by a condensation reaction with octadecanol, providing a support for hybrid lipid membranes.[24,25] In other work, 13-(chlorodimethylsilylmethyl)heptacosane was used as a hydrophobic support for a hybrid membrane.[26] In each case, a complete coating of the hydrophobic group was used, resulting in an exclusively hybrid membrane formation after exposure to lipids. Here, we utilized a mixture of hydrophilic (DETAS) and hydrophobic (ODTS) silanes to obtain heterogeneous surface coatings that template regions of both supported bilayer and hybrid membrane on the same nanoparticle.

Scheme 3. Assay for Interstitial Volume Using Melittin or Triton-X To Release Entrapped, Self-Quenching Calcein

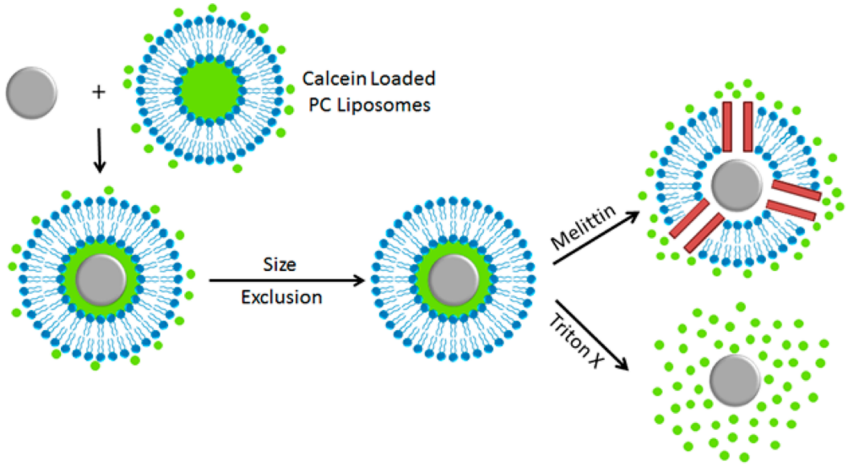

Table 4. Calculated Interstitial Water Layer Volume and Thickness

input DETAS (mol %)	calculated volume per SiNP ($\times 10^3$ nm^3)[a]	calculated water thickness (Å)[b]
100	441	89
95	372	77
88	300	65
81	240	54
73	216	50
65	156	37
39	105	25
17	53	13

[a]Calculated using eq 8. [b]Calculated using eq 10.

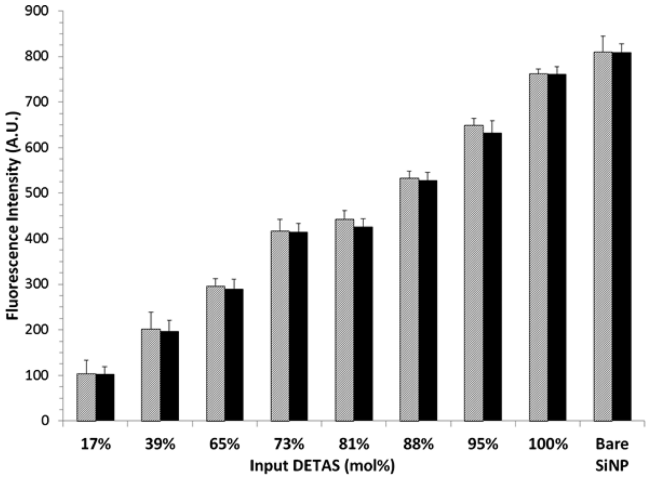

Figure 4. Interstitial volume of PC-coated SiNPs measured by fluorescence intensity. Fluorescence was measured after purification of the SiNPs and mixing with melittin (light bars) or Triton-X (dark bars). Mean ± SD, n = 5.

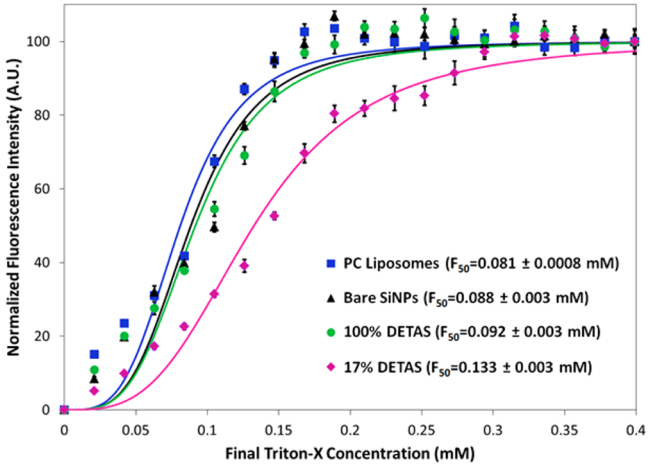

Figure 5. Fluorescence measurements to determine PC bilayer stability to Triton-X. Data were fitted with nonlinear regression, and the F_{50} values were calculated as the concentration of Triton-X that resulted in a 50% increase in fluorescence intensity. Maximum absolute fluorescence was subtracted to 0 a.u. at 0 mM and normalized to 100 a.u. at 0.4 mM. Mean ± SD, n = 5.

From this study of surface modifiers, we identified the chemical properties that are essential to preparing a mixture of supported and hybrid membranes. Initially, we used the more common silane modifier, (3-aminopropyl)triethoxysilane (APTES). However, unlike DETAS, we found that the lipid layers formed on APTES-coated SiNPs were unstable and permeable to dithionite (Supporting Information Figure S2). Previous lipid mobility measurements on APTES-modified mesoporous silica surfaces showed that APTES reduces lipid diffusion.[50] We suggest that APTES may hydrogen-bond directly to the lipids, reducing mobility. Given the importance of a hydration layer between the lipids and the substrate, we reasoned that DETAS would provide more hydration because of its having more hydrogen-bonding groups and therefore would result in better supported bilayers. One possible role of the water layer could be to extend the hydrogen bonding network that connects the lipid to the surface, and APTES may provide too direct a coupling, and DETAS creates a larger water layer. The interstitial water layer measured is higher than typical for supported bilayers and suggests that polymerized silanes on the surface result in increased porosity or void spaces. Alternatively, the SiNPs may have a rough surface that creates water-filled regions between the SiNP surface and the lipid. Another possible explanation would be multilayering of lipids with entrapped layers of water, although large regions of multilayering are ruled out by TGA analysis. ODTS was selected as a hydrophobic modifier rather than 13-(chlorodimethylsilylmethyl)heptacosane or octadecanol, which are much more and much less reactive than DETAS,

dx.doi.org/10.1021/jp308305y | J. Phys. Chem. B 2013, 117, 2113−2122

respectively. We reasoned that the methoxy and ethoxy groups on DETAS and ODTS would react at similar rates and under mild conditions, allowing for a simultaneous deposition, and that the relative input ratios of silane would determine the amount of hydrophobic and hydrophilic surface coverage.

TGA was used to confirm coating of the nanoparticles and to estimate the relative amount of each silane on the SiNP surface, similar to previous methods.[41] The weight percent loss range for SiNPs used in functionalization was equivalent to 0.97 to 2.58 silanes per silanol (Table 1) and is consistent with polymerized silanes on the surface, suggesting that no more free silanol groups are available on the surface. Although the two silanes have unique signatures in the DTA, the weight loss for each molecule occurs across a broad and overlapping temperature range. After measuring the weight loss that occurs above and below a cutoff of 440 °C, it was possible to estimate the fraction of each silane on the surface by referencing the 100% DETAS and 100% ODTS samples using eq 1. From this analysis, it can be seen that each sample is within 10% of the input ratio of silanes used (Table 1). Using different temperature cutoffs in this analysis has minimal effect on this conclusion (not shown). Given the very low water solubility and high turbidity of the 100% ODTS-functionalized SiNPs, we can rule out complete partitioning of each silane to different populations of SiNPs in the same reaction pot; if all the ODTS in the reaction added to one subset of the SiNPs, they would be insoluble. In all but one of the SiNP functionalizations, ODTS is present in a greater amount than the mole fraction of ODTS added. On average, there is 12% more ODTS on the SiNPs than would be predicted by the input mole percent. Only in the 17% DETAS sample is DETAS over-represented compared with its input mole percent. Phase separation of the two silanes during the deposition process could explain these deviations from the input ratios. Binding of ODTS to the SiNP surface above a threshold may increase the likelihood of additional ODTS binding to that SiNP. We anticipate that some degree of phase separation is likely, as depicted in Scheme 1. Heterogeneous patches of ODTS and DETAS are also reasonable on the basis of the tendency of phase separation to occur during self-assembly of hydrogen-bonding precursors[28] and are consistent with our other evidence that supported bilayers and hybrid membranes coexist on the SiNPs.

Thermal analysis of the PC-coated SiNPs supports a correlation between the fraction of hydrophobic modification and the fraction of the surface covered by a hybrid membrane. Our method for PC coating the functionalized SiNPs is similar to methods reported for coating bare or hydrophobic SiNPs.[2,26,41] After coating, each sample was isolated from free liposomes, and the quantity of PC on each SiNP was measured by TGA. The amount of PC contained on the SiNPs decreased with an increasing amount of ODTS modification, consistent with the idea that ODTS is coated by a hybrid membrane (with 1 leaflet of PC) and that DETAS is coated with a supported bilayer (with 2 leaflets of PC) (Scheme 1). By assuming that the 100% DETAS-modified SiNPs contain exclusively supported bilayers, using eq 2, it was possible to estimate the percentage of supported bilayer on each SiNP using the TGA data (Table 2). This analysis follows the same trend as the fraction of DETAS (Table 1) and is consistent with a mixture of supported and hybrid membranes on the SiNPs that is determined by the amount of ODTS available.

For all of the SiNP samples, the fraction of supported bilayer is somewhat higher than the fraction of DETAS observed by TGA (Tables 1 and 3), suggesting that the supported bilayer regions have more than a bilayer of PC associated with them. Regions of multilayered PC or attached liposomes would increase the amount of PC needed to cover the particles. If some regions of non-phase-separated ODTS and DETAS exist on the surface and they are coated with bilayer, this similarly would account for the discrepancy. Another explanation could arise from inclusion of an additional fraction of interdigitated PC that is exclusively in the outer leaflet. Such structures have been proposed for PC-coated bare SiNPs.[40,41,47] If the degree of interdigitation is determined largely by the membrane curvature, the excess PC in the outer leaflet will be similar throughout this series.

Quenching assays using NBD-PC allowed for quantification of the relative fraction of PC present in the outer and inner leaflets, providing further confirmation that supported and hybrid membrane regions coexist on each SiNP (Table 3). In contrast to using APTES as a surface modifier (Supporting Information Figure S2), the 100% DETAS-coated SiNPs form a stable and completely ion-impermeable bilayer when coated with PC (Figure 3). The NBD-PC fluorescence intensity drops by 56% after the initial introduction of dithionite and drops an additional 44% after the membrane is porated by introduction of melittin (Figure 3) or Triton-X (Supporting Information Figure S1). This difference can largely be explained by an 8 nm difference in diameter for the inner and outer leaflets that is expected for a lipid bilayer on a sphere. For example, a SiNP with a 116 nm diameter and a 9 nm water layer is expected to have an inner leaflet diameter of 134 nm with 81 000 lipids and an outer leaflet diameter of 142.2 nm with 91 000 lipids. The lipid would be distributed with 53% in the outer leaflet and 47% in the inner leaflet. Thus, our NBD-PC measurements are consistent with previous studies of NBD-PC-doped lipid bilayers that indicate no preferential distribution of NBD-PC to inner or outer bilayer leaflets.[51]

The fact that the second intensity drop after melittin addition is rapid and comparable to that induced by Triton-X suggests a substantial water layer under the lipids through which the dithionite migrates after melittin addition. The relative amount of the first NBD-PC fluorescence drop also scales with the fraction of ODTS on the SiNP surface (Table 3). As more ODTS is added, more hybrid membrane is formed. This is consistent with the ODTS-modified regions containing a hybrid membrane in which there is no inner leaflet. Therefore, all the NBD-PC is in the outer leaflet and is accessible to dithionite prior to any disruption of the membrane.[44]

The method of calculating the fraction of supported bilayer from TGA data provides results similar to the method using NBD-PC quenching. The TGA method attributes a slightly smaller fraction to being a supported bilayer than does the NBD-PC quenching method (~7% less on average). In neither case, do we account for the expected difference in size of the inner leaflet and outer leaflet, although this difference is small (~3%). In the case of NBD-PC quenching, the data do not suggest that there is a complete interdigitated bilayer of PC that would have resulted in a much larger outer leaflet fluorescence drop. Using NBD-PC to test for interdigitation is valid only if the NBD-PC partitioning is comparable to and therefore representative of the PC partitioning. The similarity of the TGA and quenching analyses suggests that the NBD-PC does not accumulate within either leaflet more than would be expected for a PC liposome of comparable size.

By entrapping a self-quenching concentration of calcein dye inside the interstitial water layer, it was possible to correlate surface functionalization with changes in interstitial volume. The volume measured for the 100% DETAS SiNPs is consistent with a 89 Å water layer (Table 4). As the hybrid fraction increases with increasing ODTS, the interstitial water layer thickness decreases, as expected. Both melittin and Triton-X release a comparable amount of calcein in each sample, supporting the idea that DETAS regions are coated with a single supported bilayer. This data also provides confirmation that the purification of PC-coated SiNPs is successful at removing free liposomes. This data provides additional support for a model with separate regions of supported and hybrid membrane (Scheme 1) in which polymerized silanes entrap more water.

One motivation for designing hybrid or tethered bilayer systems is to increase membrane stability. Here, we show improved stability for the PC-coated SiNPs that have a higher fraction of hybrid membrane. The F_{50} values for SiNPs containing 100% DETAS (0.092 ± 0.003 mM) and 17% DETAS (0.133 ± 0.003 mM) reveal that the hybrid membrane regions are significantly more stable to surfactant than the supported bilayer (Figure 5). Similarly, we have reported high stability of hybrid membranes on gold nanoparticles (using a gold etchant assay), including stability to surfactants.[21] For these heterogeneous SiNPs, any access of Triton-X through the supported bilayer regions may disrupt adjacent hybrid membrane regions, and therefore, this may not represent the highest possible stability for a hybrid membrane on SiNPs.

CONCLUSIONS

Although the surface modification necessary for supported and hybrid membranes are dissimilar, methods are reported here whereby patches of hydrophilic and hydrophobic silanes can be attached to SiNPs. These surfaces allow for templating of both supported lipid bilayers and hybrid lipid membranes on the same nanoparticle. Although planar substrates facilitate microscopic investigation of the surface heterogeneity, there are advantages to nanoparticle substrates. Here, TGA was employed to quantify the nature of the silane coating and the PC coating. Similarly, fluorescence assays were used to probe symmetry of the leaflets and volume of the interstitial layer. Ultimately, these model systems will be useful in developing an understanding of how surface anchoring alters membrane properties. In particular, this work is a substantial first step toward creating models of picket fence membrane structures, which could improve understanding of protein−membrane interactions. Because the nanoparticle size is readily tunable, it will also be possible to access different membrane curvatures, providing a mimic of biological membranes that exist at very high curvature.[52]

ASSOCIATED CONTENT

Supporting Information

Dithionite quenching assay of PC/NBD-PC coated SiNP. Dithionite quenching assay of PC/NBD-PC coated SiNP, functionalized with 100% APTES. SiNP purification study. This material is available free of charge via the Internet at http://pubs.acs.org.

AUTHOR INFORMATION

Corresponding Author

*Office: 303.556.6260. Fax: 303.556.4776. E-mail: scott.reed@ucdenver.edu.

Notes

The authors declare no competing financial interest.

ACKNOWLEDGMENTS

The authors acknowledge Dr. Min S. Wang and Reid E. Messersmith's assistance with data analysis and Heather L. Hodges for assistance with initial melittin studies. Support from NSF CBET-1033161 (SMR), NIH 2R15GM088960-02 (SMR), and a GREET award from the American Chemical Society is acknowledged.

REFERENCES

(1) Alberts, B. *Molecular Biology of the Cell*, 5th ed.; Garland Science: New York, 2008.
(2) Bayerl, T. M.; Bloom, M. *Biophys. J.* **1990**, 1−6.
(3) Johnson, S. J.; Bayerl, T. M.; McDermott, D. C.; Adam, G. W.; Rennie, A. R.; Thomas, R. K.; Sackmann, E. *Biophys. J.* **1991**, *59*, 289−294.
(4) Koenig, B.; Kruger, S.; Orts, W.; Majkrzak, C.; Berk, N.; Silverton, J.; Gawrisch, K. *Langmuir* **1996**, *12*, 1343−1350.
(5) Cremer, P.; Boxer, S. *J. Phys. Chem. B* **1999**, *103*, 2554−2559.
(6) Keller, C.; Kasemo, B. *Biophys. J.* **1998**, *75*, 1397−1402.
(7) Reviakine, I.; Brisson, A. *Langmuir* **2000**, *16*, 1806−1815.
(8) Boxer, S. *Curr. Opin. Chem. Biol.* **2000**, *4*, 704−709.
(9) Castellana, E. T.; Cremer, P. S. *Surf. Sci. Rep.* **2006**, *61*, 429−444.
(10) Vereb, G.; Szollosi, J.; Matko, J.; Nagy, P.; Farkas, T.; Vigh, L.; Matyus, L.; Waldmann, T.; Damjanovich, S. *Proc. Natl. Acad. Sci. U.S.A.* **2003**, *100*, 8053−8058.
(11) Bayley, H.; Cremer, P. *Nature* **2001**, *413*, 226−230.
(12) Parikh, A. N.; Groves, J. T. *MRS Bull* **2006**, *31*, 507−512.
(13) Bussell, S. J.; Koch, D. L.; Hammer, D. A. *Biophys. J.* **1995**, *68*, 1828−1835.
(14) Fujiwara, T.; Ritchie, K.; Murakoshi, H.; Jacobson, K.; Kusumi, A. *J. Cell. Biol.* **2002**, *157*, 1071−1081.
(15) Nicolau, D.; Burrage, K.; Parton, R.; Hancock, J. *Mol. Cell. Biol.* **2006**, *26*, 313−323.
(16) Hancock, J. *Nat. Rev. Mol. Cell. Biol.* **2006**, *7*, 456−462.
(17) Parikh, A. N. *Biointerphases* **2008**, *3*, FA22−FA32.
(18) Howland, M.; Sapuri-Butti, A.; Dixit, S.; Dattelbaum, A.; Shreve, A.; Parikh, A. *J. Am. Chem. Soc.* **2005**, *127*, 6752−6765.
(19) Plant, A. *Langmuir* **1999**, *15*, 5128−5135.
(20) Jenkins, A.; Bushby, R.; Evans, S.; Knoll, W.; Offenhausser, A.; Ogier, S. *Langmuir* **2002**, *18*, 3176−3180.
(21) Sitaula, S.; Mackiewicz, M. R.; Reed, S. M. *Chem. Commun. (Cambridge)* **2008**, 3013−3015.
(22) Kundu, J.; Levin, C. S.; Halas, N. J. *Nanoscale* **2009**, *1*, 114−117.
(23) Yang, J. A.; Murphy, C. J. *Langmuir* **2012**, *28*, 5404−5416.
(24) Koole, R.; van Schooneveld, M. M.; Hilhorst, J.; Castermans, K.; Cormode, D. P.; Strijkers, G. J.; de Mello Donegá, C.; Vanmaekelbergh, D.; Griffioen, A. W.; Nicolay, K.; Fayad, Z. A.; Meijerink, A.; Mulder, W. J. M. *Bioconjugate Chem.* **2008**, *19*, 2471−2479.
(25) Linseisen, F. M.; Hetzer, M.; Brumm, T.; Bayerl, T. M. *Biophys. J.* **1997**, *72*, 1659−1667.
(26) Wang, L.-S.; Wu, L.-C.; Lu, S.-Y.; Chang, L.-L.; Teng, I.-T.; Yang, C.-M.; Ho, J.-A. A. *ACS Nano* **2010**, *4*, 4371−4379.
(27) Geissler, M.; Xia, Y. *Adv. Mater.* **2004**, *16*, 1249−1269.
(28) Smith, R.; Lewis, P.; Weiss, P. *Prog. Surf. Sci.* **2004**, *75*, 1−68.
(29) Duschl, C.; Liley, M.; Corradin, G.; Vogel, H. *Biophys. J.* **1994**, *67*, 1229−1237.
(30) Han, X.; Critchley, K.; Zhang, L.; Pradeep, S. N. D.; Bushby, R. J.; Evans, S. D. *Langmuir* **2007**, *23*, 1354−1358.

(31) Jenkins, A.; Boden, N.; Bushby, R.; Evans, S.; Knowles, P.; Miles, R.; Ogier, S.; Schonherr, H.; Vancso, G. *J. Am. Chem. Soc.* **1999**, *121*, 5274−5280.
(32) Lenz, P.; Ajo-Franklin, C.; Boxer, S. *Langmuir* **2004**, *20*, 11092−11099.
(33) Jung, M.; Vogel, N.; Köper, I. *Langmuir* **2011**, *27*, 7008−7015.
(34) Mackiewicz, M. R.; Ayres, B. R.; Reed, S. M. *Nanotechnology* **2008**, *19*, 115607.
(35) Stöber, W.; Fink, A.; Bohn, E. *Colloids Surf.* **1968**, 62−69.
(36) Liu, J.; Jiang, X.; Ashley, C.; Brinker, C. J. *J. Am. Chem. Soc.* **2009**, *131*, 7567−7569.
(37) *Colloidal Silica: Fundamentals and Applications*, 1st ed.; Bergna, H., Roberts, W. O., Hubbard, A., Eds.; CSC Press: Boca Raton, 2005.
(38) Chan, C. C. P.; Choudhury, N. R.; Majewski, P. *Colloids Surf. A* **2011**, *377*, 20−27.
(39) Dayani, Y.; Malmstadt, N. *Langmuir* **2012**, *28*, 8174−8182.
(40) Ahmed, S.; Nikolov, Z.; Wunder, S. L. *J. Phys. Chem. B* **2011**, *115*, 13181−13190.
(41) Ahmed, S.; Wunder, S. L. *Langmuir* **2009**, *25*, 3682−3691.
(42) Bhalla, A.; Chicka, M. C.; Tucker, W. C.; Chapman, E. R. *Nat. Struct. Mol. Biol.* **2006**, *13*, 323−330.
(43) Ningsih, Z.; Hossain, M. A.; Wade, J. D.; Clayton, A. H. A.; Gee, M. L. *Langmuir* **2012**, *28*, 2217−2224.
(44) Zeineldin, R.; Piyasena, M. E.; Sklar, L. A.; Whitten, D.; Lopez, G. P. *Langmuir* **2008**, *24*, 4125−4131.
(45) Ladokhin, A. S.; Selsted, M. E.; White, S. H. *Biophys. J.* **1997**, *72*, 1762−1766.
(46) Edwards, D. A.; Prausnitz, M. R.; Langer, R.; Weaver, J. C. *J. Controlled Release* **1995**, *34*, 211−221.
(47) Savarala, S.; Ahmed, S.; Ilies, M. A.; Wunder, S. L. *Langmuir* **2010**, *26*, 12081−12088.
(48) Mornet, S.; Lambert, O.; Duguet, E.; Brisson, A. *Nano Lett.* **2005**, *5*, 281−285.
(49) Basit, H.; Van der Heyden, A.; Gondran, C.; Nysten, B.; Dumy, P.; Labbé, P. *Langmuir* **2011**, *27*, 14317−14328.
(50) Worsfold, O.; Voelcker, N. H.; Nishiya, T. *Langmuir* **2006**, *22*, 7078−7083.
(51) Bhalla, A.; Chicka, M. C.; Tucker, W. C.; Chapman, E. R. *Nat. Struct. Mol. Biol.* **2006**, *13*, 323−330.
(52) Zimmerberg, J.; Kozlov, M. M. *Nat. Rev. Mol. Cell. Biol.* **2006**, *7*, 9−19.